PHOTOELECTRIC SETTING TECHNIQUE FOR FRINGES OF EQUAL THICKNESS

By P. E. CIDDOR*

[Manuscript received 12 June 1973]

Abstract

A theoretical and experimental study has been made of the photoelectric setting technique for fringes of equal thickness. The predicted departures of the theory from that for fringes of equal inclination have been confirmed and the parameters suitable for various practical applications have been calculated.

I. INTRODUCTION

Photoelectric scanning interferometers have been used with remarkable success in the precise measurement of wavelengths (Baird and Smith 1960; Bruce and Hill 1961). The principle of a scanning interferometer is that the optical path difference is varied sinusoidally and the modulated flux is detected photoelectrically and then analysed into its harmonic components. The vanishing of the component at the scanning frequency is taken to define a setting on a fringe maximum. Figure 1 is a schematic diagram of an interferometer of this type. The limits to the precision of this method of measurement have been calculated by Hanes (1959, 1963) and by Hill and Bruce (1962, 1963). The specific instruments to which these calculations referred were the Fabry–Perot interferometer and its two-beam analogue the Michelson interferometer. It was assumed that settings were always made on a fringe maximum, by changing the mean separation of the oscillating interferometer, as is usual in precise interferometry.

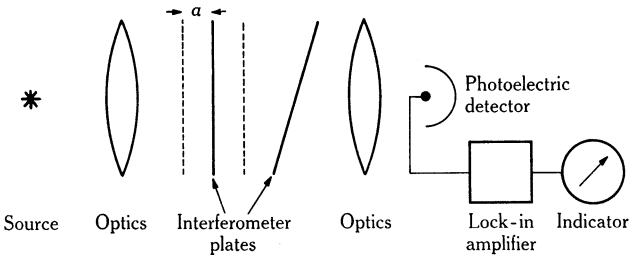

Fig. 1.—Schematic diagram of a scanning interferometer.

In the present paper the above calculations are extended to the case of Fizeau-type interferometers, in which interference fringes of equal thickness are used. The application of photoelectric scanning to such interferometers would increase the accuracy and convenience of many metrological observations. The term "Fizeau

* Division of Applied Physics, National Standards Laboratory, CSIRO, City Road, Chippendale, N.S.W. 2008.

interferometer" is used here to describe any instrument in which localized fringes of equal thickness are produced, and therefore includes the Twyman–Green and Kösters modifications of the Michelson interferometer. Following Hanes (1959, 1963) and Hill and Bruce (1962, 1963), the limiting precision of setting is considered in terms of the ratio of the signal to the shot noise in the photoelectric detector. The theory for the Haidinger fringe case (Fabry–Perot interferometer) is first summarized briefly and some of the results are quoted for reference and comparison.

Raymond (1970) has considered a particular application of the scanning technique to a Kösters interferometer of the type used in metrology. His analysis is directed to the problem of the optimum conditions of operation for a given plate separation. On the other hand, Raymond considers several topics which are not covered in the present paper, namely the effect of dark current in the photodetector, the relative merits of setting on dark two-beam fringes or bright fringes, and the difference between operation with variable slit width and with variable fringe spacing. Where Raymond's treatment overlaps the present work, full agreement is found.

II. Haidinger Fringe System

The intensity distribution function for multiple-beam fringes is described by the Airy function, which may be written in the form given by Krebs and Sauer (1953):

$$I(n) = Z\left(1 + 2\sum_{k=1}^{\infty} G_k \cos 2\pi kn\right), \tag{1}$$

where

$$Z = T^2/(1-R^2), \qquad G_k = R^k \exp(-\pi^2\mu^2k^2/4\ln 2),$$

T and R are the transmittance and reflectance of the interferometer plates respectively, n is the order of interference, and $\mu = 2t\Delta\sigma = n\Delta\sigma/\sigma$, $2t$ being the optical path difference, σ the wave number of the spectral line, and $\Delta\sigma$ its full width at half intensity. The distribution of power available in the interference pattern is given by the product of this distribution function and the total power available in one order of interference. Hanes (1959) showed that the power per order is given by

$$p_H = \pi^2 D^2 L Z_0/4t\sigma, \tag{2}$$

where L is the radiance of the source, Z_0 the transmittance of the external optics, and D the diameter of the illuminating beam.

Hanes (1959, 1963) and Hill and Bruce (1962, 1963) have used equations (1) and (2) to derive expressions for the signal and noise currents in a photodetector, with particular reference to settings on a fringe maximum and to the use of the fundamental component of the modulated signal. The corresponding equations for the general case of setting at any order N, including the possibility of using various harmonics of the modulated signal, are set out below.

The mean current i_0 is given by

$$i_0 = 2p_H bZ\{1 + 2\sum G_k J_0(2\pi ka)(2\pi kb)^{-1} \sin 2\pi kb \cos 2\pi kN\}\theta e/hc\sigma, \tag{3}$$

while the fundamental component i_1 and the second harmonic i_2 of the difference

signal for offset of δN orders are

$$i_1 = 8p_H Z\{\sum G_k J_1(2\pi ka)\sin 2\pi kb\cos 2\pi kN\}(\theta e/hc\sigma)\delta N \quad (4)$$

and

$$i_2 = 8p_H Z\{\sum G_k J_2(2\pi ka)\sin 2\pi kb\sin 2\pi kN\}(\theta e/hc\sigma)\delta N, \quad (5)$$

where $2b$ is the range of orders accepted by the aperture of the detector, a is the amplitude of oscillation, $N = 2t\sigma$ is the mean order over the aperture, δN is a small offset from the setting N, $J_m(x)$ is a Bessel function of the first kind of order m and argument x, θ is the quantum efficiency of the detector, and e is the electronic charge. The shot noise in the detector is given by

$$i_n = (2ei_0\,\mathrm{d}\nu)^{\frac{1}{2}}, \quad (6)$$

$\mathrm{d}\nu$ being the detector bandwidth. Substitution for i_0 from equation (3) then yields the noise current in the form

$$i_n = e(4p_H bZv_0\,\theta\,\mathrm{d}\nu/hc\sigma)^{\frac{1}{2}}, \quad (7)$$

where v_0 is the term enclosed in braces in (3). The signal-to-noise ratio for the fundamental signal is therefore

$$r_1 = i_1/i_n = 8u_1(p_H Z\theta/4bv_0\,hc\sigma\,\mathrm{d}\nu)^{\frac{1}{2}}\delta N, \quad (8)$$

where u_1 is the term in braces in (4). Equation (8) may be written in the form used by Hanes (1959, 1963) and Hill and Bruce (1962, 1963), namely

$$r_1 = \left(64\,\theta\tau\frac{p_H}{2hc}\frac{Z}{\sigma}\frac{u_1^2}{v}\right)^{\frac{1}{2}}\delta N, \quad (9)$$

where $\tau = 1/\mathrm{d}\nu$ and $v = 2bv_0$. Similar expressions involving u_2, u_3, etc. apply for higher harmonic terms. Substitution of equation (2) into (9) finally gives the expression

$$r_1 = \left(\frac{\pi^2 D^2}{2hc}Z_0\,\theta\tau\frac{L}{\Delta\sigma}\right)^{\frac{1}{2}}\left(32\mu Z\frac{u_1^2}{v}\right)^{\frac{1}{2}}\frac{\delta N}{N} \quad (10)$$

$$= \Delta^{\frac{1}{2}}\Phi_1\,\delta N/N, \quad (11)$$

where Δ is an "interferometer constant" and Φ_1 is the noise factor (Hill and Bruce 1962).

III. Fizeau Fringe System

(a) *Basic Relations*

The relations for the multiple-beam Fizeau system differ from those for the Haidinger system because the power p_F available per order of interference is different. The form of the calculation of the signal and noise currents is the same, however, since it follows from the form of the Airy function.

In Figure 2, a source of radiance L and area A, which is assumed to be sufficiently small not to affect the coherence of the light, is at the focus of a lens of focal length f

and diameter D. The amount of power in the collimated beam is given by

$$LA\pi D^2/4f^2 .$$

This power is distributed uniformly over an area $\frac{1}{4}\pi D^2$ and so the power per unit area (the irradiance) is $LA/f^2 = L\Omega$, where Ω is the solid angle subtended by the source at the lens. The interference pattern will consist of linear fringes, the spacing of which will depend on the angle α between the plates but not on their separation t. This characteristic of Fizeau fringes has a significant effect on the calculation of p_F.

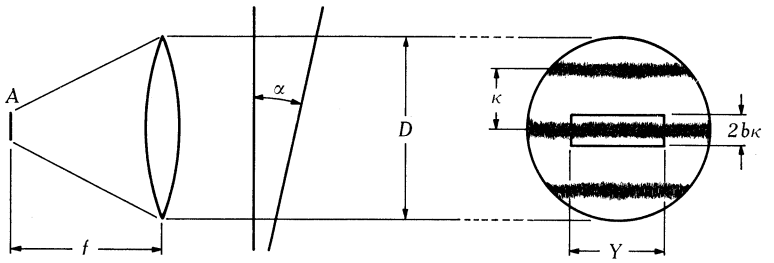

Fig. 2.—Photometric parameters of a Fizeau interferometer: A is the area of the source, D and f are the diameter and focal length of the lens, α is the angle between the plates, Y is the width of the detecting aperture, and κ is the spacing of the fringes.

The detecting aperture will be a rectangle of some convenient length Y and width $X = 2b$ fringe spacings. In practice the fringes will be projected into the aperture by an auxiliary optical system but initially we shall assume that the aperture is located in the plane of the fringes (i.e. between the plates). The geometric spacing of the fringes will be $\lambda/2\alpha$, so that one order of interference will occupy an area $Y\lambda/2\alpha$ or $Y/2\alpha\sigma$. The power incident in this area, allowing for a transmittance factor Z_0 in the external optics, will be

$$p_F = Z_0 L\Omega Y/2\alpha\sigma . \tag{12}$$

Equation (12) may be contrasted with the corresponding relation (2) for Haidinger rings. If we now substitute p_F as given by (12) for p_H in equation (9), and use the identity

$$\frac{1}{\sigma^2} = \frac{1}{\sigma^2}\frac{4t^2\Delta\sigma^2}{4t^2\Delta\sigma^2} = \frac{\mu^2}{N^2\Delta\sigma^2},$$

we obtain the result

$$r_1 = \left(\frac{\Omega Y}{\alpha}\frac{1}{2hc} Z_0\theta\tau\frac{L}{\Delta\sigma^2}\right)^{\frac{1}{2}}\left(32\mu^2 Z\frac{u_1^2}{v}\right)^{\frac{1}{2}}\frac{\delta N}{N} \tag{13}$$

$$= \delta^{\frac{1}{2}}\phi_1\,\delta N/N, \tag{14}$$

where we have used lower case Greek letters to distinguish quantities relevant to the Fizeau interferometer. There are several important differences between equations

(13) and (10):

(i) The radiometric properties of the source enter as $L/\Delta\sigma^2$, rather than as $L/\Delta\sigma$. Consequently the remarks of Hill and Bruce (1962) and Hanes (1963) about the ineffectiveness of narrowing the bandwidth of the source are not applicable. Instead, the precision would increase if both L and $\Delta\sigma$ were reduced in the same proportion.

(ii) The angular size Ω of the source is significant. An upper limit to this quantity is set by the requirement that the coherence should be sufficiently high for visual alignment.

(iii) The noise function ϕ_1 depends on μ rather than on $\mu^{\frac{1}{2}}$.

The numerical values of δ and Δ, and also of ϕ_1 and Φ_1, turn out to be comparable for practical interferometers.

(*b*) *Limiting Precision of Setting*

Following the previous work of Hanes (1959) and Hill and Bruce (1962), we define the limiting precision as $N/\delta N$, where δN is that value which makes the ratio r_1 equal to unity,

$$N/\delta N = \Delta^{\frac{1}{2}}\Phi_1 \qquad \text{(Haidinger)} \tag{15a}$$

or

$$N/\delta N = \delta^{\frac{1}{2}}\phi_1 \qquad \text{(Fizeau)}. \tag{15b}$$

Bell (1960) has demonstrated that values of $N/\delta N$ calculated in this way should be reduced by 30% to allow for secondary emission noise in a photomultiplier.

Hill and Bruce (1962) showed that, for a typical Fabry–Perot interferometer, detector, and isotopic light source, Δ would be about 5×10^{19} and that the maximum attainable value of Φ_1 was about 0·6. The resultant limiting precision was $(5\times10^{19})^{\frac{1}{2}}\times0{\cdot}6/1{\cdot}3$, or about $3{\cdot}2\times10^9$. For comparison we may consider a Fizeau interferometer with the following parameters:

$$\Omega = \pi r^2/f^2 = \pi\beta^2 = 10^{-6}\pi,$$

for a source aperture of radius r and angular radius $\beta = 10^{-3}$ rad; $\alpha = 6\times10^{-5}$ rad, corresponding to a 5 mm fringe spacing; $Y = 25$ mm, corresponding to one-half of a 50 mm field (this choice of Y assumes that the field of view contains two sets of fringes, as will frequently be the case for Fizeau fringes); and also

$$Z_0 = 0{\cdot}2, \qquad \theta = 0{\cdot}07, \qquad \tau = 1\text{ s},$$

$$L = 0{\cdot}3\text{ W m}^{-2}\text{ sr}^{-1}\text{ (606 nm line of }{}^{86}\text{Kr)}, \qquad \Delta\sigma = 1{\cdot}3\text{ m}^{-1}.$$

These values yield the result

$$\delta = 8\times10^{18}.$$

We shall find in the following subsection that ϕ_1 can be as large as 0·3 for multiple-beam Fizeau fringes, giving a limiting precision of $(8\times10^{18})^{\frac{1}{2}}\times0{\cdot}3/1{\cdot}3 = 6{\cdot}5\times10^8$, which is comparable with the value for the Haidinger case. The magnitude of δ can

be varied by a factor of about 10 with the particular choice of Y and α. The ultimate lower limit to α is set by the finite size of the field of view. The detecting aperture cannot be wider than D, so that, since $2b$ is equal to the ratio of the aperture size to the fringe spacing, we must have

$$2b < D/(2\alpha\sigma)^{-1}, \qquad \text{or} \qquad \alpha > b/D\sigma.$$

The corresponding precision would be about five times greater than was calculated for $\alpha = 6\times10^{-5}$ rad. A somewhat higher limit to α is set by the practical need to have at least two fringes in the field of view in order to ensure that they are aligned parallel to the aperture.

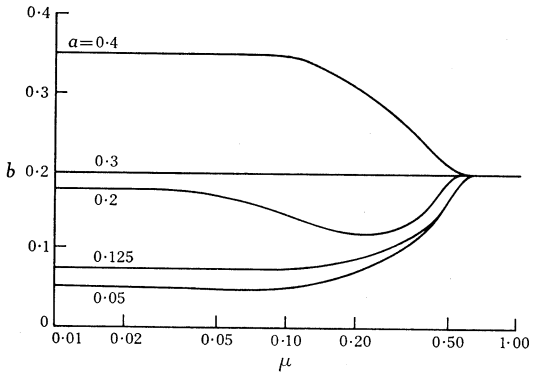

Fig. 3.—Optimum half-aperture b as a function of μ for five values of the amplitude a of a scan.

(c) *Results of Calculations of Noise Functions*

The noise function ϕ_1 has been calculated for a wide range of values of the parameter μ. From equations (10) and (13) we have

$$\phi_1 = \mu^{\frac{1}{2}}\Phi_1,$$

and since this equation does not involve R, a, or b explicitly their optimum values will be the same for Fizeau and Haidinger fringes. Figure 3, which is an extended version of Figure 11 of Hill and Bruce (1962), shows the optimum value of b for each choice of a and μ. The optimum value of a for multiple-beam fringes is 0·125 for values of μ up to 0·15, and 0·3 for larger μ. (Because of the rapid convergence of all the Fourier series for large values of μ, the multiple-beam case reduces to the two-beam one, for which the optimum value of a is 0·3, independent of μ.) Hill and Bruce (1963) showed that for multiple-beam fringes the best value of R was 0·73, and this value has been used throughout the present calculations. For the two-beam case R should be 1·0.

Figures 4(*a*) and 4(*b*) show a selection of the calculated results for multiple-beam and two-beam fringes respectively. In each figure, curve H is the ideal noise function Φ_1 for Haidinger fringes and curve F is the corresponding function ϕ_1 for Fizeau fringes, the functions having been optimized at each value of μ by adjustment of the parameters a and b. It can be seen that the peaks are shifted to larger values of μ for the Fizeau fringes, and that the best values of ϕ_1 are within a factor of two of the best

values of Φ_1. (The other curves and the experimental points in these figures are discussed in Section V.)

The two-beam interferometers are marginally superior to the multiple-beam instruments, for both types of fringe, but the large values of μ would present mechanical problems in a Michelson interferometer. Although the optimum values of a are rather large, detailed calculations show that ϕ_1 remains within 10% of its peak value for a as small as 0·1, with b in the range 0·1–0·3. Raymond (1970) has pointed out that, for two-beam fringes of high visibility, setting on a dark fringe improves the signal to noise ratio by as much as a factor of two. This advantage is rapidly lost as the visibility falls below about 0·5.

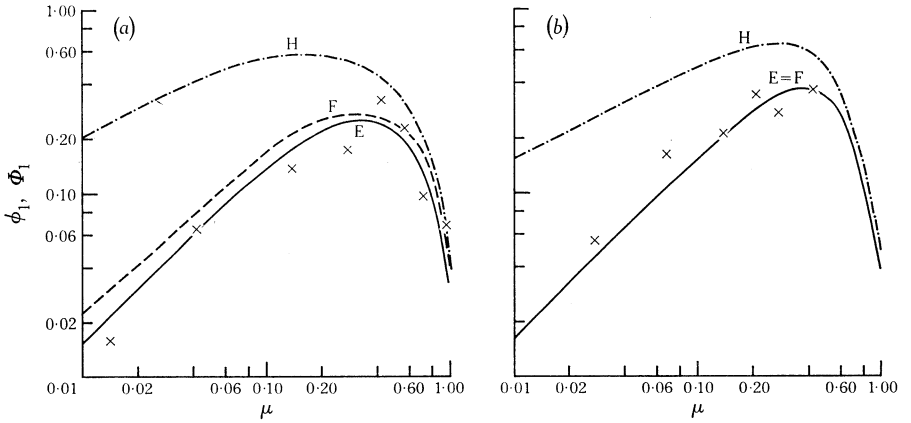

Fig. 4.—Noise functions versus μ for (*a*) multiple-beam fringes and (*b*) two-beam fringes. The curves H and F are the ideal noise functions Φ_1 and ϕ_1 for Haidinger and Fizeau fringes respectively, and have been obtained by optimizing a and b at each value of μ. The theoretical curves E are the calculated functions for Fizeau fringes with the experimental parameter values (*a*) $a = b = 0{\cdot}2$ and (*b*) $a = 0{\cdot}3$, $b = 0{\cdot}2$. Curve E is identical with the optimum curve F for two-beam fringes. The points show the experimental results for the precision, scaled to the corresponding E curve.

IV. Effects of Departures from Ideal Geometry

The theory presented so far has assumed that the detecting aperture conforms exactly to the shape of the fringes. In spectroscopic instruments it is possible to ensure that this is so to a very high degree of accuracy, since the optical surfaces can be made flat to 0·01 fringe so that the fringe pattern is circular (Haidinger) or linear (Fizeau) to a corresponding degree, while the alignment of the surfaces and of the aperture to the fringes also can be carefully controlled to an adequate degree. In the metrology of practical end-standards of length, on the other hand, we are faced with three departures from ideal geometry:

(i) the surfaces are not optically smooth, but show scratches of various depths and widths which are left by the lapping process and by subsequent wringing of the surfaces;

(ii) the surfaces commonly depart from flatness by as much as 0·2 fringe, and sometimes by as much as 0·5 fringe on longer standards;

(iii) it is not possible to make the end faces perfectly parallel, which means that the fringe pattern from the end of the standard will not be parallel to that from the base plate to which the standard is wrung and consequently that an aperture cannot be aligned simultaneously with both patterns.

The effects of surface roughness are to reduce the visibility of the interference pattern and to slightly change the mean order of interference (averaged over a region that is large compared with the scale of the roughness). These effects have been discussed by Hill (1963) and will not be considered further here.

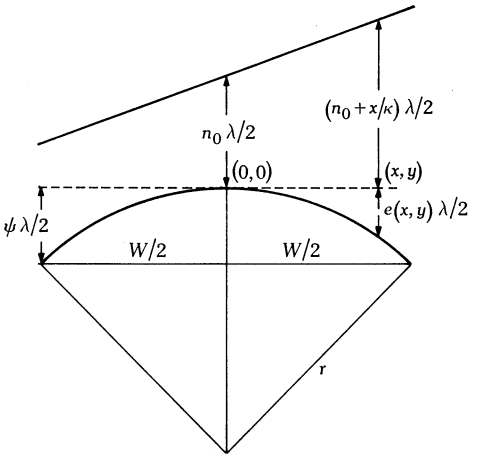

Fig. 5.—Geometry of a wedge interferometer: n_0 is the order of interference at the centre of the aperture and $e(x, y)\,\lambda/2$ represents the departure from ideal fringe spacings at the point (x, y).

Suppose that ideally the two surfaces of a two-beam Fizeau-type interferometer form a wedge, oriented so that straight fringes lie along the y direction and have spacing κ in the x direction. The irradiance in the interference pattern is given by

$$I(n) = Z(1 + V_0 \cos 2\pi n), \tag{16}$$

where n is the order of interference, Z the transmittance of the interferometer, and V_0 the visibility of the fringes, which depends on path difference, line width, source size, etc. The order of interference at any point in the aperture is

$$n(x, y) = n_0 + x/\kappa, \tag{17}$$

$n_0 = n(0, 0)$ being the order at the centre. We shall describe any departure from this ideal geometry by a function $e(x, y)$, where $e(x, y)\,\lambda/2$ is the difference between the actual and ideal spacings at (x, y) (see Fig. 5). The full expression for $n(x, y)$ therefore becomes

$$n(x, y) = n_0 + x/\kappa + e(x, y). \tag{18}$$

The result of integrating over the aperture is

$$F(n_0) = XYZ\{1 + V_1 \cos 2\pi(n_0 - \Delta N)\}, \tag{19}$$

where X and Y are the dimensions of the aperture (in units of κ),

$$V_1 = V_0(B^2+C^2)^{\frac{1}{2}}/XY, \qquad \Delta N = (2\pi)^{-1}\arctan(-C/B), \tag{20}$$

with

$$B = \int_S \cos 2\pi\{x/\kappa + e(x,y)\}\,\mathrm{d}S, \qquad C = \int_S \sin 2\pi\{x/\kappa + e(x,y)\}\,\mathrm{d}S, \tag{21}$$

S being the area of the aperture.

A comparison between equations (16) and (19) shows that the effect of an error $e(x,y)$ is simply to change the visibility and introduce a phase shift ΔN. The subsequent calculations of signal strengths and limiting precisions are unaffected in form and only the numerical results are altered, to an extent that is dependent on the characteristics of $e(x,y)$. Several general comments may be made at once. If $e(x,y)$ is antisymmetric about $(0,0)$, the integral C in (21) vanishes and therefore ΔN is zero. This will be the case, for example, when the interferometer surfaces are tilted about the y axis and the fringes are not parallel to the aperture. If $e(x,y)$ vanishes everywhere, C again vanishes and V_1/V_0 reduces to the $(\sin x)/x$ function that is characteristic of slit apertures. In general ΔN will not vanish but will be a correction to the apparent order of interference, analogous to that which arises in a Haidinger system.

To proceed further it is necessary to assume a specific form for $e(x,y)$. A simple model, which is roughly descriptive of a typical end-standard, is a spherical cap of geometric radius r, for which the sagittal depth at (x,y) is approximately given by

$$e(x,y)\,\lambda/2 = (x^2+y^2)/2r.$$

The evaluation of the integrals B and C in (21) involves straightforward but extensive expansions of the trigonometric functions and leads to expressions involving Fresnel integrals. Only some of the results will be indicated here. It is convenient to express these results as functions of the spherical error ψ, defined as $e(0,\frac{1}{2}W)$ where W is the geometric width of the end-standard in the y direction. This form accords with the practical assessment of the flatness error of an end-standard. The relation between ψ and r is

$$\psi \approx W^2/4\lambda r.$$

The noise function ϕ_1 for a two-beam Fizeau system has been calculated for various values of the spherical error. The results confirm the intuitive expectation that Y should generally be as large as possible, to increase the amount of usable light. However, for severe errors ($\psi \sim 0{\cdot}5$) the rapid decrease in visibility as Y is increased overcompensates for the gain in signal, and the noise function decreases when Y exceeds $0{\cdot}75\,W$. For moderate values of ψ ($\leqslant 0{\cdot}2$), the visibility remains as high as $0{\cdot}7\,V_0$ even when $Y = W$.

The optimum value of X is found to be $0{\cdot}4$, which agrees with the result $2b = 0{\cdot}4$ for the ideal case when $\psi = 0$. The optimum scan amplitude remains close to $a = 0{\cdot}3$. The variation of the noise function ϕ_1 with ψ under these conditions is shown in Figure 6. The curve for V_1/V_0 is virtually identical with that for ϕ_1 because the Bessel function in equation (3) is small and the dominant term in ϕ_1 is u_1 and hence

V_1 (see equation (4)). The loss in precision is not very severe for practical values of ψ; for example, an end-standard of rather poor flatness ($\psi = 0{\cdot}2$) would still allow 93% of the ideal precision of setting. Rather surprisingly, the variation of ϕ_1 with ψ is practically independent of the fringe spacing κ. It is therefore desirable to use as large a fringe spacing as possible, subject to the requirements mentioned above that the orientation of the fringes should be observable. A practical point here is that there is generally a narrow boundary region on an end-standard where there is pronounced curvature, and this region, which could be 10% of W, should be excluded from the aperture.

The phase shift, or aperture correction term ΔN, also varies little with the fringe spacing. It is independent of the actual order of interference because it is the result of integrating over a given fringe pattern, no matter how that pattern is generated. (This is in contrast to the usual correction for the integration over the entrance aperture, which does depend on n_0.)

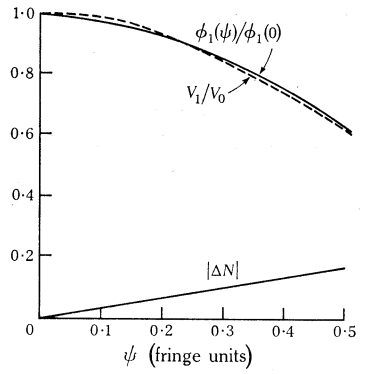

Fig. 6.—Effects of increasing spherical error ψ on the noise function $\phi_1(\psi)$, visibility V_1, and aperture correction ΔN (in fringe units) for the optimum conditions $a = 0{\cdot}3$, $X = 0{\cdot}4$, and $Y = W$.

Since the spherical error ψ, as defined above, is positive for a convex surface, while the mean length of an end-standard with a convex surface is less than its defined length at the centre of the surface, a positive correction to the length is required when ψ is positive. The converse is true for a concave surface. If the base plate supporting the end-standard is curved, the preceding rule is applicable in reverse, but in practice base plates are of such quality that no correction is necessary.

The geometric defect (iii) referred to above was the relative misalignment of the aperture and the fringes. Goldberg and Brockman (1962) showed that the photoelectric visibility and signal to noise ratio in this case depend on the function

$$\frac{\sin 2\pi X}{2\pi X}\,\frac{\sin 2\pi Y}{2\pi Y},$$

where X and Y are the aperture dimensions relative to one fringe spacing. The phase shift is zero because of the antisymmetry of the arrangement. Goldberg and Brockman showed that some advantage could be gained by using a circular aperture instead of a rectangular one, because of the reduced loss in photoelectric visibility as the fringes rotated. The optimum diameter of the aperture was shown to be 0·59 fringe.

V. Experimental Tests of Theory

The Fabry–Perot interferometer described by Bruce and Hill (1961) and Hill and Bruce (1962) was modified for the present work. Initially the plates were adjusted to produce Fizeau fringes in transmission, which were projected onto an adjustable slit in front of the photomultiplier. The light source was a cooled electrodeless ^{198}Hg lamp with a filter to isolate the 546 nm radiation. The output of the photomultiplier was synchronously detected. The decade fringe-controller (Bruce and Hill 1961) was calibrated as usual by setting on successive fringe maxima.

The technique adopted for determining the precision of setting on a fringe differed from that used previously. The time constant of the detecting system (τ in the theoretical equations) was objectively defined by setting the filter on the d.c. output of the lock-in amplifier to 1 s. A digital voltmeter was set to sample and display the output once each 5 or 10 s (sampling time 0·1 s). The sole function of the observer was to record the displayed readings, so that no subjective integration was involved. The controller was set to 0·01–0·02 fringe from a peak and five voltmeter readings were taken. The controller was then adjusted by 0·01 or 0·02 fringe and five more readings were taken. Alternate groups of readings made in this way were used to construct two drift lines of detector output against time. (It was assumed that, for these small offsets, the detector output would be proportional to the fringe offset.) Each drift line was fitted by a least-squares straight line, and the difference between the intercepts, combined with the prior calibration of the controller, gave the scale factor (volts per fringe). The uncertainty of setting (δN) was taken to be the standard deviation of the residuals of the observed points about the fitted line. The *precision* of setting was taken as before to be $N/\delta N$, with N the order of interference.

Suppose that the drift lines at controller settings C_1 and C_2 are

$$v_1 = m_1 t + c_1 \qquad \text{and} \qquad v_2 = m_2 t + c_2,$$

with standard deviations σ_1 and σ_2 respectively. In this case

$$(c_2 - c_1)\,(\text{volt}) \equiv (C_2 - C_1)/C\,(\text{fringe}),$$

where C controller units correspond to one fringe, and therefore

$$\sigma\,(\text{volt}) \equiv \delta N = \frac{C_2 - C_1}{C}\,\frac{\sigma}{c_2 - c_1}\,(\text{fringe}).$$

A typical set of results is shown in Figure 7, where it can be seen that the difference between the intercepts is not much larger than the scatter of the points. Consequently the calculated values of δN show considerable scatter.

The experimental values of $N/\delta N$ were compared with theory in the following way. The theoretical noise function was calculated for the experimental values of a and b. (For the multiple-beam experiment it was convenient to fix each of these at 0·2 instead of optimizing them at each value of μ, while, for the two-beam experiment, the constant optimum values $a = 0{\cdot}3$ and $b = 0{\cdot}2$ were used.) A polynomial approximation was found for each curve. In Figure 4(*a*) the curve E shows this

polynomial; in Figure 4(*b*) the polynomial is identical with the optimum curve F. Each set of values of $N/\delta N$ was then fitted to its appropriate polynomial by adjusting a scaling factor. The factor which yielded the closest fit was taken as the experimental value of $\delta^{\frac{1}{2}}$. The quality of the fits may be seen from Figure 4. The multiple-beam results (*a*) have their peak at the theoretical value of μ and fit the curve reasonably well. The two-beam results (*b*) were restricted to $\mu = 0{\cdot}42$ by mechanical limitations when the interferometer was converted to a Michelson system, but the peak appears to be in the expected region.

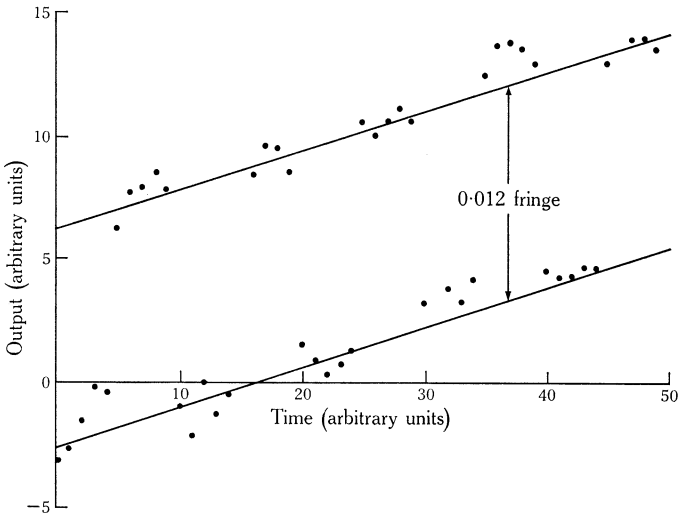

Fig. 7.—Typical plot of detector output against time as used in the determination of the experimental precision of setting.

The experimental values of $\delta^{\frac{1}{2}}$ found by the above method were

$$\text{multiple beam} \quad 2{\cdot}61 \times 10^8 ; \qquad \text{two beam} \quad 2{\cdot}23 \times 10^8 .$$

The interferometer constants used here differed somewhat from the values adopted in the earlier work. In particular, the effective transmittance of the external optics was very low ($<0{\cdot}002$), largely because of considerable overfilling of the various apertures and also because of losses in auxiliary components such as windows and relay optics. After including rough estimates for these losses together with a correction for the different radiance and quantum efficiency of the mercury green radiation, the resulting estimates of $\delta^{\frac{1}{2}}$ were

$$\text{multiple beam} \quad 23{\cdot}69 \times 10^8 ; \qquad \text{two beam} \quad 18{\cdot}18 \times 10^8 ;$$

i.e. respectively $9{\cdot}1$ and $8{\cdot}2$ times the corresponding experimental values. Considering the very approximate nature of the estimates of Z_0 and the sensitivity of the signal to slight errors in the alignment of the fringes, this degree of agreement is thought to be satisfactory. Certainly the functional form of the experimental graphs is in accordance with the theory and the peak values occur near the predicted values of μ.

VI. Discussion

(*a*) *Practical Metrology with Large Two-beam Interferometers, using Thermal Sources of Light*

The practical problem that gave rise to this work was to extend photoelectric setting techniques to Michelson interferometers, which are used to calibrate line- and end-standards of length (Bruce 1956; Ciddor and Bruce 1967). In such instruments the optical separation t between the two mirrors may be as large as 0·25 m. The field of view generally contains two sets of fringes, the relative displacement of which must be measured to obtain the length of the standard. At such large mirror separations, the visibility is poor and visual observations are difficult and prone to error. Direct estimation of fringe fractions is limited to an accuracy of 0·05 fringe, but the use of a compensator or half-shade device can improve this to 0·01–0·02 fringe.

Because of the division of the field, the quantity Y which was introduced in Section III must be less than one-half the diameter of the field (in fact Y should preferably be about 0·8 of this limit, as mentioned in Section IV). It has been shown in Section IV that even quite substantial errors in flatness (up to 0·2 fringe) produce a very slight loss in precision and that misalignment errors, although more serious, can be adequately controlled. The major limitation is the large value of μ, which can reach 0·6–0·8 for values of t up to 0·25 m. These values are well beyond the peak of the curve of ϕ_1 versus μ and lead to ϕ_1 values of 0·1–0·25, compared with a peak of 0·38. Using $\delta \approx 2\times10^{18}$ and $\delta N = 0{\cdot}01$ with $N = 10^6$, we find

$$r = \delta^{\frac{1}{2}}\phi_1\,\delta N/N \approx \sqrt{2\times10^{9}\times0{\cdot}2\times10^{-8}} \approx 3\,.$$

(*b*) *Practical Metrology with Large Two-beam Interferometers, using Laser Light*

The use of highly coherent light leads to fringes of high visibility. The narrow bandwidth of the laser affects both δ and ϕ_1 as follows.

A typical helium–neon laser has a power output of 1 mW into a cone of semi-angle 3×10^{-4} rad from a surface of diameter 2 mm. The radiance L is therefore 10^9 $\mathrm{W\,m^{-2}\,sr^{-1}}$, compared with 0·3 $\mathrm{W\,m^{-2}\,sr^{-1}}$ for the krypton 606 nm radiation. The relative spectral width is very small; even if we allow for broadening of the line by thermal and mechanical instabilities, we can reasonably expect to have $\Delta\sigma/\sigma = 10^{-9}$, or $\Delta\sigma = 1{\cdot}6\times10^{-3}$ $\mathrm{m^{-1}}$ for the 633 nm radiation. The parameter $L/\Delta\sigma^2$ is therefore 4×10^{14} $\mathrm{W\,sr^{-1}}$ (c.f. 0·18 $\mathrm{W\,sr^{-1}}$ for krypton 606 nm) and $\delta^{\frac{1}{2}}$ is increased to $4{\cdot}7\times10^7$ times the value for krypton 606 nm radiation.

The small value of $\Delta\sigma$ leads to a very small value of μ. Taking $t = 0{\cdot}25$ m we find $\mu = 0{\cdot}0008$. Now for $\mu < 0{\cdot}15$, a very good approximation to ϕ_1 in Figure 4(*b*) is $\phi_1 = 1{\cdot}58\,\mu$. This linear relation is to be expected from the form of equation (13), since both u and v tend to unity as μ tends to zero. Substituting $\mu = 0{\cdot}0008$ in the expression for ϕ_1 we obtain $\phi_1 = 0{\cdot}0013$. The precision is therefore

$$N/\delta N = 4{\cdot}7\times10^{7}\times(2\times10^{18})^{\frac{1}{2}}\times0{\cdot}0013 = 8{\cdot}6\times10^{13}\,.$$

In practice it would be necessary to attenuate and diffuse the beam, but it is clear that the precision far exceeds any practical requirement.

(c) *Precise Refractometry of Gases*

An accurate measurement of the refractive index of air is an essential part of interferometric metrology. The usual way of determining the refractive index is to measure the difference between the optical lengths of two geometrically equal cells, one in air and the other in vacuum (Terrien 1965). The two paths are usually placed side by side in one or both arms of a Michelson interferometer so that the actual optical path differences between the interfering beams can be made very small. If the order of interference in the path containing the vacuum cell is made equal to zero, the corresponding value of μ is zero. The optical length of the air cell is $(n-1)d$ greater than that of the vacuum cell, where n is the refractive index and d the common geometric length. For a cell 0·3 m long, which is a practical size, and $n = 1{\cdot}000\,276$ approximately, the value of μ is about 0·0005 for a relatively broad spectral line (cadmium 644 nm, $\Delta\sigma = 3{\cdot}3\ \mathrm{m}^{-1}$).

The noise function ϕ_1 (Fig. 4(*b*)) decreases almost linearly with μ, as mentioned above, and the calculated value of ϕ_1 at $\mu = 0{\cdot}0005$ is 0·0008, giving a precision of

$$N/\delta N = \delta^{\frac{1}{2}}\phi_1/1{\cdot}3 = 8{\cdot}59\times 10^5.$$

Since $N = 2(n-1)d/\lambda$ is only about 250, δN can be determined to about 0·0003 fringe, corresponding to $\delta n/n = 3\times 10^{-10}$. This far exceeds practical requirements, but of course we have used an optimistic value of δ based on a high value of Z_0.

VII. Acknowledgments

The author is grateful to Mr. R. M. Duffy for substantial assistance with the electronics, and to Dr. C. F. Bruce for discussions.

VIII. References

Baird, K. M., and Smith, D. S. (1960).—*P.-v. Séanc. Com. int. Poids Més.* **28**, 121.
Bell, D. A. (1960).—"Electrical Noise." (D. Van Nostrand: London.)
Bruce, C. F. (1956).—*J. scient. Instrum.* **33**, 478.
Bruce, C. F., and Hill, R. M. (1961).—*Aust. J. Phys.* **14**, 64.
Ciddor, P. E., and Bruce, C. F. (1967).—*Metrologia* **3**, 109.
Goldberg, J. L., and Brockman, R. H. (1962).—*Electron. Technol.* p. 140.
Hanes, G. R. (1959).—*Can. J. Phys.* **37**, 1283.
Hanes, G. R. (1963).—*Appl. Optics* **2**, 465.
Hill, R. M. (1963).—*Optica Acta* **10**, 141.
Hill, R. M., and Bruce, C. F. (1962).—*Aust. J. Phys.* **15**, 194.
Hill, R. M., and Bruce, C. F. (1963).—*Aust. J. Phys.* **16**, 282.
Krebs, K., and Sauer, A. (1953).—*Annln. Phys.* **13**, 354.
Raymond, O. J. (1970).—*Appl. Optics* **9**, 1140.
Terrien, J. (1965).—*Metrologia* **1**, 80.